



Investigation of Solar Proton Access Into the Inner Magnetosphere on 11 September 2017

Murong Qin¹, Mary Hudson^{1,2}, Brian Kress³, Richard Selesnick⁴, Miles Engel⁵, Zhao Li¹, and Xiaochen Shen⁶

Key Points:

- Pulse height analyzed data from the Van Allen Probes REPT instrument is compared with model solar proton geomagnetic cutoffs
- The Dartmouth cutoff code is extended to calculate cutoff energy for particles arriving from arbitrary directions at the spinning spacecraft
- Geosynchronous transfer orbit measurements and calculated cutoff extend models previously applied to low-altitude and geosynchronous cutoffs

Correspondence to:

M. Qin,
murong.qin.gr@dartmouth.edu

Citation:

Qin, M., Hudson, M. K., Kress, B. T., Selesnick, R., Engel, M., Li, Z., & Shen, X. (2019). Investigation of solar proton access into the inner magnetosphere on 11 September 2017. *Journal of Geophysical Research: Space Physics*, 124, 3402–3409. <https://doi.org/10.1029/2018JA026380>

Received 7 DEC 2018

Accepted 12 APR 2019

Accepted article online 23 APR 2019

Published online 27 MAY 2019

¹Department of Physics and Astronomy, Dartmouth College, Hanover, NH, USA, ²High Altitude Observatory, National Center for Atmospheric Research, Boulder, CO, USA, ³Cooperative Institute for Research in Environmental Sciences, University of Colorado Boulder, Boulder, CO, USA, ⁴Space Vehicles Directorate, Air Force Research Laboratory, Kirtland AFB, NM, USA, ⁵Space Science and Application, Los Alamos National Laboratory, Los Alamos, NM, USA, ⁶Center for Space Physics, Boston University, Boston, MA, USA

Abstract In this study, access of solar energetic protons to the inner magnetosphere on 11 September 2017 is investigated by computing the reverse particle trajectories with the Dartmouth geomagnetic cutoff code (Kress et al., 2010). The maximum and minimum cutoff rigidity at each point along the orbit of Van Allen Probe A is numerically computed by extending the code to calculate cutoff rigidity for particles coming from arbitrary direction. Pulse height analyzed (PHA) data have the advantage of providing individual particle energies and effectively excluding background high-energy proton contamination. This technique is adopted to study the cutoff locations for solar protons with different energy. The results demonstrate that cutoff latitude is lower for solar protons with higher energy, consistent with low-altitude vertical cutoffs. Both the observations and numerical results show that proton access into the inner magnetosphere depends strongly on angle between particle arrival direction and magnetic west. The numerical result is approximately consistent with the observation that the energy of almost all solar protons stays above the minimum cutoff rigidity.

1. Introduction

While being significantly more stable compared to the highly variable outer radiation belt dynamics (Baker et al., 2007; Miyoshi et al., 2001; Shen et al., 2017), inner zone proton fluxes can show rapid loss during storm time and trapping during solar proton events (Hudson et al., 1997; Selesnick et al., 2010; Zou et al., 2011) besides gradual solar cycle variations (Li et al., 2001; Selesnick et al., 2007; Qin et al., 2014). Also, solar proton access to the inner magnetosphere and the proton trapping mechanism are not yet well understood.

Solar proton events consist of energetic protons emitted from the Sun or accelerated by interplanetary shocks. Solar protons are shielded by the Earth's magnetic field in the inner magnetosphere. Whether a proton is able to penetrate the Earth's magnetic field depends on its magnetic rigidity (momentum per unit charge). The cutoff rigidity is the threshold below which the proton fluxes are zero due to magnetic shielding. Each geographic location and particle arrival direction corresponds to a specific cutoff rigidity (Störmer, 1955), with the maximum cutoff rigidity when protons arrive from approximately the east and minimum cutoff rigidity when they come from approximately the west (Rodriguez et al., 2010), determined by whether the center of gyro motion is inside or outside of the point of observation. Most previous studies focus on investigating the geomagnetic cutoff invariant latitude at low Earth orbit (Kress et al., 2010; Leske et al., 2001). The difference in SEP cutoffs is small for protons coming from different directions at high latitudes because of their small gyroradius. Kress et al. (2004) examined solar proton access to the inner magnetosphere using observation from a highly elliptical orbit satellite. This study was limited to a single energy channel and an investigation of the cutoff for solar protons arriving from near magnetic west.

The two Van Allen Probe spacecraft, with their orbit across a range of L shells between 1.1 and 5.8 R_E near the equatorial plane (10.2° inclination), provide an opportunity to investigate the cutoff energies for protons at different altitude over much of the inner magnetosphere. These fast rotating stable inertial spinners (nominally at 5 rpm) allow detection of particle flux arriving from a broad range of directions every 11 s. In order to understand how deep into the magnetosphere protons with different energies and different

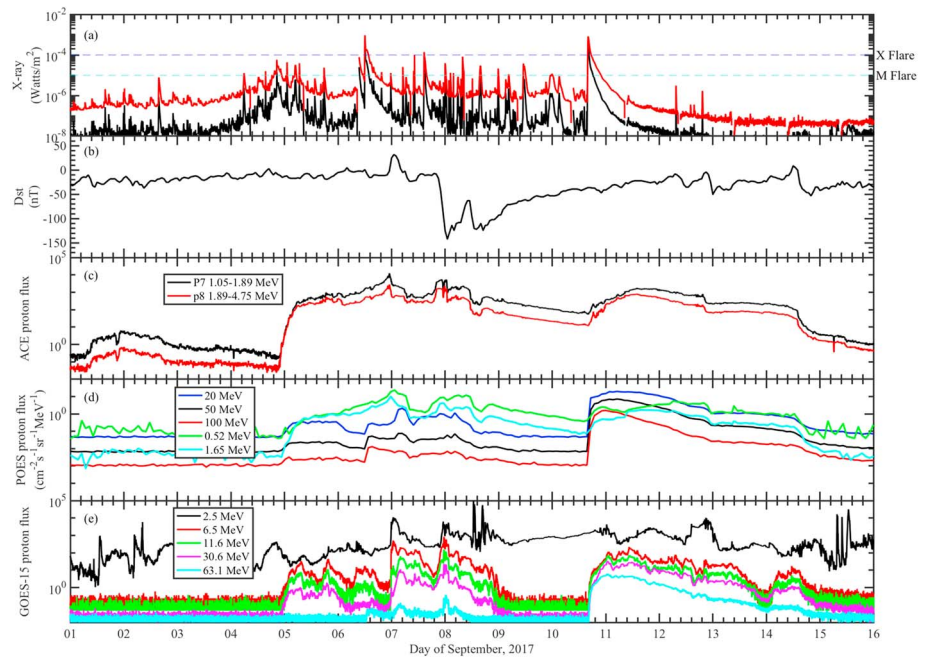


Figure 1. (a) X-rays short and long wavelength channel irradiance (0.05–0.4 nm, black; 0.1–0.8 nm, red) (b) *Dst* index (c) ACE/EPAM Solar Energetic Particle ACE LEMS120 P7p and P8p energy channel. (d) Averaged flux in every orbit beyond $L \sim 15$ measured by POES satellites. (e) GOES-15 flux in west field of view. Panels (c), (d) and (e) are shown without intercalibration to summarize interplanetary, low-altitude, and geosynchronous observations. ACE = Advanced Composition Explorer; POES = Polar Orbiting Environmental Satellite; GOES-15 = Geostationary Operational Environmental Satellite-15.

directions can penetrate, we investigate the geomagnetic cutoff of solar protons during geomagnetic quiet conditions for the 10–14 September 2017 solar proton event associated with an X-class solar flare and coronal mass ejection (CME)-producing active region with interplanetary shock observed at STEREO-A and Mars which missed the Earth (Luhmann et al., 2018). There was no accompanying geomagnetic storm, unlike the SEP event which accompanied the 6–8 September CME shock-driven geomagnetic storm. The penetration of >60-MeV protons into the magnetosphere during the 10–12 September 2017 solar energetic particle event was explored with the Relativistic Proton Spectrometer (Mazur et al., 2013) onboard Van Allen Probes (O'Brien et al., 2018). Lower-energy solar protons with higher intensity can also cause serious space weather hazards and are thus deserving further attention. In our study, we focus on solar protons with energy from 20 to 200 MeV with measurements from the Relativistic Electron Proton Telescope (REPT; Baker et al., 2013) from the Energetic Particle, Composition, and Thermal Plasma Suite (Spence et al., 2013) on Van Allen Probes. The primary REPT science data provide energy bin count rates reported to the spacecraft once each spin. Each spin is subdivided into 36 equal duration sectors. It consists of counts of particle events in 20 energy bins that are classified by 20 logic statements, eight of which are proton energy bin logic statements. Contamination in the proton low energy channels must be addressed here since they have some response to high-energy protons. As solar proton flux level gets lower when penetrating further into the magnetosphere, the high-energy background protons which come from outside the field of view of the detector may dominate the flux level at the inner boundary of the solar protons and thus can cause misinterpretation of the cutoff location. Logic equations have been improved but can only eliminate part of the background contamination. The secondary REPT science product is a sampling of PHA data sets. Each packet consists of 100 PHA data sets, and each set is for a single particle event (Baker et al., 2013). Analysis tools which use PHA data were developed by Selesnick (2014) and Selesnick et al. (2018) to eliminate the background contamination for inner-belt measurements (Selesnick et al., 2014, 2016, 2018). This method has been shown not only to successfully eliminate background contamination but also to provide accurate incident kinetic energy of each individual proton, allowing us to analyze the detailed dependence of cutoff locations on proton energy. We will briefly introduce this tool in section 2. Details of this method can be found in Selesnick et al. (2017).

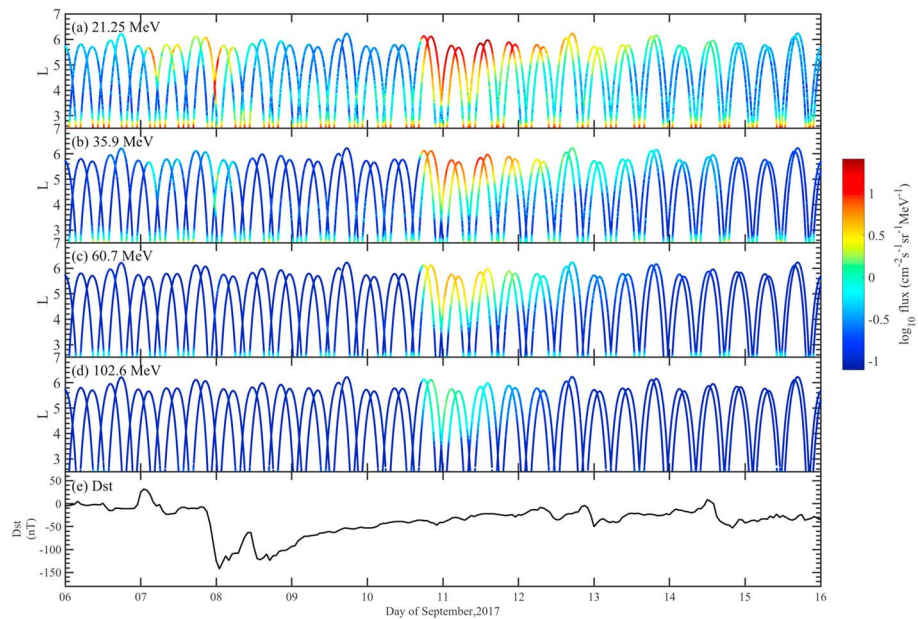


Figure 2. Level 2 proton flux in four energy channels (a) 21.25 MeV, (b) 35.9 MeV (c) 60.7 MeV (d) 102.6 MeV of the Relativistic Electron Proton Telescope instrument on Van Allen Probes A and B covering two solar energetic proton events in September 2017. *Dst* is shown in the bottom panel (e).

In this paper, cutoff locations determined from spin sector-resolved flux and PHA event data are compared. Numerical cutoff calculations are performed, and a comparison is made between observations and simulation results.

2. Observations of Solar Proton Events

2.1. Overview of Solar Proton Events

Figure 1 is an overview of the solar proton events in September 2017, which contained two characteristic SEP event types. The first beginning late on 5 September was accompanied by arrival of a CME shock and ensuing geomagnetic storm with minimum $Dst = -124$ nT on 8 September. The second and stronger SEP event which produced a Ground Level Event signature without a geomagnetic storm was observed beginning on 10 September (O'Brien et al., 2018). Proton measurements by interplanetary Advanced Composition Explorer (c), low-altitude Polar Orbiting Environmental Satellite (d), and Geostationary Operational Environmental Satellite-15 (e) along with geosynchronous X-ray measurements (a) and the *Dst* index (b) are shown in Figure 1. Measurements from both Polar Orbiting Environmental Satellite and Geostationary Operational Environmental Satellite-15 satellites are at high *L* with little geomagnetic shielding effect. Measurements from Van Allen Probes with geosynchronous transfer orbit will be adopted to investigate the geomagnetic shielding effect inside the magnetosphere.

2.2. REPT Data Analysis

The two Van Allen Probes are equipped with a variety of wave and particle instruments, which can be used to study radiation belt dynamics. Both Van Allen Probe spacecraft have the spin axes pointed generally in the direction of the Sun. The REPT instrument measures both energetic electrons and protons. In REPT Level-2 (L2) output, the measured count rates are corrected for background and dead time effect and then converted to physical flux units. Both spin-averaged differential flux and spin sector-resolved differential flux with 36 equal angular sectors per spin are provided. Figure 2 shows the spin-averaged proton flux in four energy channels (a) 21.25 MeV, (b) 35.9 MeV, (c) 60.7 MeV, and (d) 102.6 MeV of the REPT instrument on Van Allen Probes A and B covering two SEP events in September 2017 with REPT L2 data. We are concentrating on the second event, starting near the end of 10 September 2017.

Figure 3 shows the spin sector-resolved flux for (a) 21.25-MeV, (b) 35.9-MeV, (c) 60.7-MeV, and (d) 102.6-MeV protons observed by Van Allen Probe A on 11 September 2017. The inner radiation belt trapped

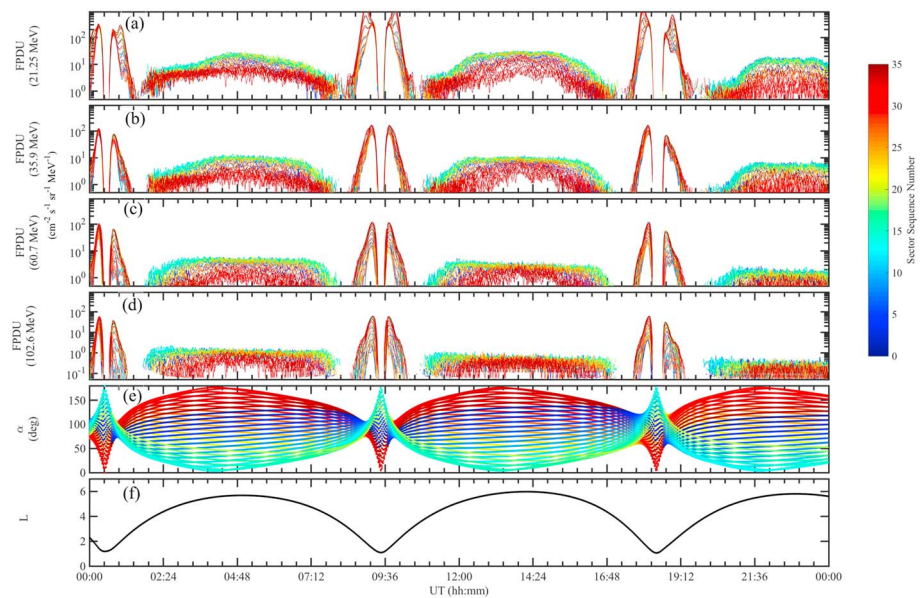


Figure 3. The spin sector-resolved unidirectional differential proton flux (FPDU) in 36 angle bins for (a) 21.25-MeV, (b) 35.9-MeV, (c) 60.7-MeV, and (d) 102.6-MeV protons observed by Van Allen Probe A on 11 September 2017. Different colors represent flux for different sectors. (e) The angle α between particle arrival direction and magnetic west. Each color corresponds to the value from the same detector as the above four panels. (f) L value of the spacecraft.

protons are at lower L ($L < 3$), and the solar protons are at higher L . Different colors represent flux for different sectors. Each sector measures flux for protons arriving from different angles α between particle arrival direction and magnetic west, which is shown in Figure 3e. Magnetic west is defined as the direction perpendicular to the satellite position vector and the dipole axis in SM coordinates. The particle arrival direction is approximately the same as the center of REPT pointing direction (half-angle of REPT acceptance cone is 16°), which is $(x, y, z) = (-0.15643446, -0.98768834, 0.)$ in spacecraft coordinates and can be converted to SM coordinates with satellite attitude in SM coordinates.

It can be seen from Figure 3 that fluxes at high L are different in different spin sectors corresponding to different look directions in panels (a)–(d). This can be explained by the fact that protons arriving from the west have gyro centers above the spacecraft, while those arriving from the east have gyro centers below the spacecraft where their flux is reduced by additional geomagnetic shielding (Kress et al., 2013; Rodriguez et al., 2010). Thus, it is to be expected that the sectors with higher flux levels measure particles with smaller α , the angle between magnetic west and particle arrival direction. It is also seen that the flux for protons with larger α decreases more rapidly than for smaller α as the spacecraft goes further into the magnetosphere at high L , demonstrating that protons with larger α in a given energy channel are more strongly shielded than those with smaller α by the magnetic field as they get closer to the Earth. For minimum α (corresponding to sectors of green lines), the solar proton flux in the 21.25-MeV energy channel increases with L value and peaks at apogee. However, in the higher energy channels (panels b–d), the proton flux has a wider flat top distribution along L in the outer radiation belt, indicating that the proton energy in those channels with minimum α is above the corresponding cutoff energy. Thus, those protons in the higher energy channel from a given direction are not shielded by the magnetic field. This further demonstrates that cutoff rigidity depends strongly on the direction from which protons arrive (Kress et al., 2013; Rodriguez et al., 2010).

It appears in Figure 3 that particles identified as solar protons in the lower energy channels (panels a and b) penetrate even deeper into the inner magnetosphere than the higher-energy protons (panels c and d). This may be due to two reasons. The first reason is that the low energy channels are more susceptible to contamination from high-energy background protons, so they show additional counts at locations where only the high energies are above cutoff. The second issue is an overcorrection for instrumental dead time in L2 data caused by high trapped electron intensity that may occur concurrently with the solar proton

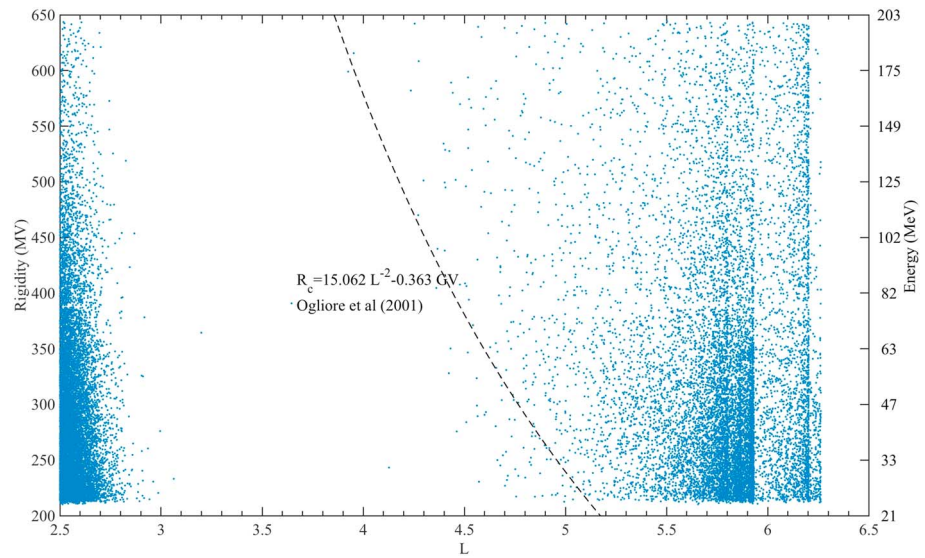


Figure 4. The rigidity of measured pulse height event data as a function of L from 10 to 12 September 2017. The dashed line plots cutoff locations for solar protons with different energy from the empirical model of Ogliore et al. (2001). Roughly three 9-hr orbits per day result in a different apogee in consecutive orbits when mapped to L due to rotation of the Earth's dipole axis evident in distinct apogee cutoffs at high L .

measurements near cutoff, leading again to a false proton intensity. The correction for high electron intensity could be adjusted, but we have not done so because we would still have the problem with contamination of higher-energy protons.

Applying a probabilistic approach to the PHA data, the high-energy contamination can be effectively eliminated (Selesnick, 2014). The REPT PHA data for a single incident particle consist of nine digital numbers in the nine aligned silicon detectors. Each data number can be converted to the energy deposited in each detector. For an incident proton with a certain energy and incidence angle, the probable energy deposited in a path length of material satisfies a proton straggling function. Thus, the probability density can be obtained by substituting the incident energy in each detector, incident angle, and energy deposited in each detector into the proton straggling function (Selesnick, 2014). If the probability density is lower than the minimum threshold value 10^{-3} , then the particle is considered as a proton incident from outside the field of view or an electron and is excluded (Selesnick et al., 2017). This tool has been shown to effectively eliminate the contamination from high-energy background protons and has been applied to study the dynamics of the protons in the inner radiation belt (Selesnick et al., 2014, 2016, 2018). In this work, this method is adopted to investigate the cutoff rigidity of solar protons for the first time.

Applying the above probabilistic approach to the PHA data on 10–12 September 2017, valid proton measurements are selected. Here the proton energies are converted to rigidity and the rigidity of each measured proton is shown versus L in Figure 4. Note that density of points on the plot is not representative of proton intensity because it depends on the varying intensity of the outer zone electrons, the time spent at each L , and the different upper L limits for each orbit. The outer limit of trapped protons is below $L = 3$ and the dots outside $L = 3$ are solar protons. It can be seen that the cutoff location for solar protons has a clear dependence on the proton energy, with higher-energy protons reaching closer to the Earth as expected. To test cutoff locations for solar protons, here we adopted the relationship, R (in GV) = $15.062L^{-2} - 0.363$, between vertical cutoff rigidity and the McIlwain L parameter, which has been applied to describe geomagnetic cutoff for cosmic rays with rigidities from 500 to 1,700 MV in Ogliore et al. (2001). It is seen that the dashed line in Figure 4 roughly describes the relationship between cutoff energy and the cutoff location but with some of the dots below the dashed line at lower rigidity (energy). These dots below the dashed line may be the protons arriving from the direction with angle greater than 90° with respect to west and thus have rigidity lower than the vertical cutoff rigidity.

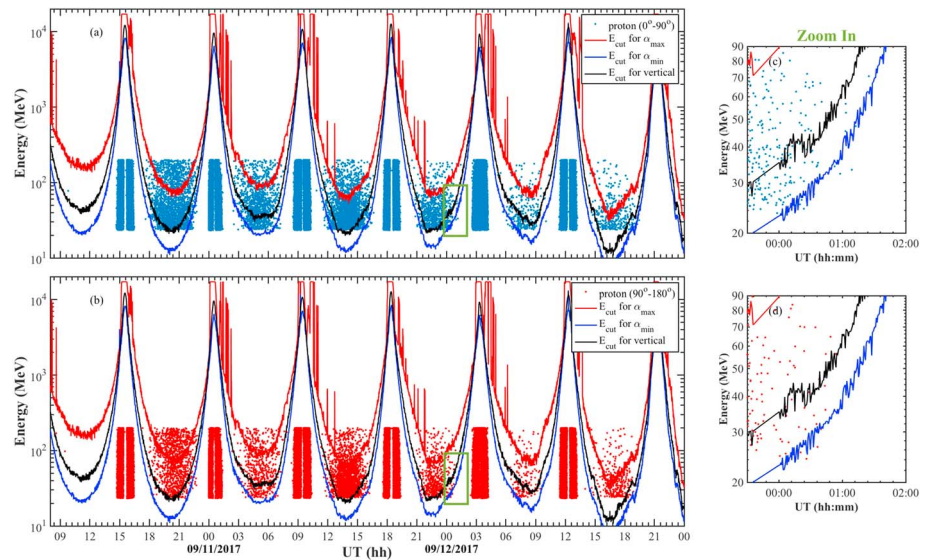


Figure 5. (a) Valid PHA proton events with protons arriving from 0° to 90° with respect to magnetic west (blue dots). (b) Valid PHA proton events with protons arriving from 90° to 180° with respect to magnetic west (red dots). The days are for September 2017. The cutoff energy for protons arriving from directions with angles of α_{\min} (solid blue line), α_{\max} (solid red line) with respect to magnetic west are computed. The black solid line is cutoff energy for protons arriving from the vertical direction. Vertical thick blue and red stripes at perigee correspond to trapped protons in the inner radiation belt. (c, d) The zoom in of the rectangular regions in panels (a) and (b), respectively.

3. Simulation

To quantify solar proton access into the inner magnetosphere, we numerically calculated the solar proton cutoff rigidity along the trajectories of the Van Allen Probes spacecraft on 11 September 2017 with the Dartmouth geomagnetic cutoff code (Kress et al., 2010). This is achieved by computing the time reversed particle trajectory in the TS05 geomagnetic field model (Tsyganenko & Sitnov, 2005) combined with IGRF model. A particle which comes from a certain direction and of a certain rigidity is launched at a location along the orbit. If the particle can escape the magnetosphere, then a viable trajectory can be found, indicating that the particle's rigidity exceeds the cutoff rigidity at that location. An automated numerical search algorithm is adopted to locate the cutoff rigidity (see Kress et al., 2010 for more detailed description). The result is shown in Figure 5. The effect of penumbral shielding of protons by the Earth, which creates an obstacle to access, is evident in sharply increased spikes near perigee (Kress et al., 2015). The red (blue) lines in both panels represent the maximum (minimum) cutoff energy (E_{cut}) for protons arriving from the direction with maximum (minimum) angle α with respect to west, as determined by the REPT look direction as the spacecraft spins. Note that the detector may not view all possible directions over 4π sr, only the ones that the sensor might sample during a spin given the satellite's instantaneous spin axis direction. The black lines represent the cutoff energy for protons coming from the vertical direction. The blue dots in Figure 5a represent the valid PHA proton events with protons arriving from 0° to 90° with respect to magnetic west and red dots in Figure 5b represent valid PHA proton events with protons arriving from 90° to 180° with respect to magnetic west. The lower and upper energy limits for red and blue dots are 20 and 200 MeV, respectively. It is noticed that the calculated cutoff energy (E_{cut}) for protons with α_{\max} is well above the cutoff energy (E_{cut}) for protons with α_{\min} . This is consistent with the observation in Figure 3 that larger α corresponds to lower flux level. It is also demonstrated that the energies of almost all the valid solar protons are above the minimum cutoff energy. Figures 3c and 3d expand 3a and 3b to show more clearly that almost all westward (blue) dots have higher rigidity than the westward cutoff and fewer protons access the detector from eastward (red) with gyrocenters at lower altitude where solar proton flux decreases. Theoretically, protons arriving from 90° to 180° with respect to magnetic west should have their energy above the vertical cutoff energy (black line) and most do. However, some of the red dots stay below the black line in Figure 5d. Thus, the model may overestimate the cutoff energy as found in previous studies (Kahler & Ling, 2002; Kress et al., 2010, 2013).

4. Discussion and Conclusions

In this study, access of solar energetic protons to the inner magnetosphere on 10–12 September 2017 is investigated by comparing observations from the REPT instrument onboard Van Allen Probes and numerical simulation results using the Dartmouth cutoff code (Kress et al., 2010).

Because of limited measurements near the equatorial plane, most previous studies have focused on investigating the geomagnetic cutoff invariant latitude at low Earth orbit (Kress et al., 2010; Leske et al., 2001). The difference in solar energetic proton (SEP) cutoffs is small for protons coming from different directions at high latitude because of their small gyroradius. There is also a lack of direct evidence in SEP observations to show the dependence of the cutoff location on the proton energy because of low-energy resolution in measurements and a steep gradient in cutoff with respect to latitude in LEO near the cutoff for SEP energies. High-energy resolution measurements of SEP cutoffs across a broad range of L shells near the equatorial plane are now available with the launch of Van Allen Probes.

The two Van Allen Probes with their geosynchronous transfer orbit provide measurements over much of the inner magnetosphere. The fast rotating stable inertial spinners allow detection of particle flux arriving from a broad range of directions. Both L2 flux measurements converted from primary science telemetry and secondary product of PHA data are adopted to examine the factors that may have influence on cutoff locations during geomagnetic quiet conditions. A clear dependence of the cutoff locations on the angle α between particle arrival direction and magnetic west can be seen from REPT L2 spin sector-resolved flux measurements (divided into 36 sectors in one rotation) in Figure 3. But due to overcorrection for instrumental dead time in the L2 output and contamination from high-energy background protons, cutoff locations for solar protons in the lower energy channels may appear to be even closer to the Earth than the higher-energy protons as seen in Figure 3. In order to eliminate the effect of the high-energy proton contamination, a probabilistic approach to the PHA data developed by Selesnick (2014) and Selesnick et al. (2018) is adopted. A well-defined dependence of the cutoff location on the proton energy can be obtained by analyzing Level 1 PHA data, as shown in Figure 4.

The cutoff location is also numerically simulated by computing the reverse particle trajectories. The maximum and minimum cutoff rigidity at each point along the orbit of Van Allen Probe A is numerically computed by extending the code to calculate cutoff rigidity for particles coming from arbitrary directions. The numerical result is approximately consistent with the observation that the energy of almost all solar protons stays above the minimum cutoff rigidity but may overestimate the cutoff energy in the vertical direction as found in previous studies (Kahler & Ling, 2002; Kress et al., 2010, 2013).

While this study is focused on the solar proton event of 10–12 September 2017 which occurred during geomagnetically quiet conditions, the data source and analysis approach can be applied to further study the cutoff rigidity for protons during storm conditions. An in-depth study will be performed in future work to determine the cutoff suppression, which measures the weakening of magnetic shielding due to the diamagnetic effect of ring current buildup (Leske et al., 2001) and test the correlation between geomagnetic cutoff and Dst index, which is evident in Figure 2 for the 7–8 September 2017 event. We plan to examine SEP trapping seen in the earlier SEP event (Hudson et al., 2019) and the associated formation of new ion belts (Hudson et al., 1997, 2004), well below the normal SEP cutoff (Kress et al., 2005; Lorentzen et al., 2002) during storm conditions.

Acknowledgments

This work was supported by NSF grant AGS-1455470. We would like to acknowledge high-performance computing support provided by NCARs Computational and Information Systems Laboratory. The attitude of the spacecraft can be obtained online (https://emfisis.physics.uiowa.edu/local/rbsp_att.html), and the pulse height analysis data can be obtained online (https://rbsp-ect.newmexicoconsortium.org/data_prot/rbspa/rept/level1/pha/int/2017/).

References

- Baker, D., Kanekal, S., Horne, R., Meredith, N., & Glauert, S. (2007). Low-altitude measurements of 2–6 MeV electron trapping lifetimes at $1.5 \leq L \leq 2.5$. *Geophysical Research Letters*, *34*, L20110. <https://doi.org/10.1029/2007GL031007>
- Baker, D. N., Kanekal, S. G., Hoxie, V. C., Batiste, S., Bolton, M., Li, X., et al. (2013). The Relativistic Electron-Proton Telescope (REPT) instrument on board the Radiation Belt Storm Probes (RBSP) Spacecraft: Characterization of Earth's radiation belt high-energy particle populations. *Space Science Reviews*, *179*(1), 337–381. <https://doi.org/10.1007/s11214-012-9950-9>
- Hudson, M. K., Elkington, S. R., Lyon, J. G., Marchenko, V. A., Roth, I., Temerin, M., et al. (1997). Simulations of radiation belt formation during storm sudden commencements. *Journal of Geophysical Research*, *102*(A7), 14,087–14,102. <https://doi.org/10.1029/97JA03995>
- Hudson, M., Kress, B., Mazur, J., Perry, K., & Slocum, P. (2004). 3D modeling of shock-induced trapping of solar energetic particles in the Earth's magnetosphere. *Journal of Atmospheric and Solar-Terrestrial Physics*, *66*(15), 1389–1397. <https://doi.org/10.1016/j.jastp.2004.03.024>
- Hudson, M., Qin, M., Kress, B., Li, Z., & Selesnick, R. (2019). Investigation of solar proton access into the inner magnetosphere 11 September 17. AGU Chapman Conference Abstracts.

- Kahler, S., & Ling, A. (2002). Comparisons of high latitude $E > 20$ MeV proton geomagnetic cutoff observations with predictions of the SEPTR model. *Annales Geophysicae*, 20, 997–1005. <https://doi.org/10.5194/angeo-20-997-2002>
- Kress, B., Hudson, M., Perry, K., & Slocum, P. (2004). Dynamic modeling of geomagnetic cutoff for the 23–24 November 2001 solar energetic particle event. *Geophysical Research Letters*, 31, L04808. <https://doi.org/10.1029/2003GL018599>
- Kress, B. T., Hudson, M. K., Selesnick, R. S., Mertens, C. J., & Engel, M. (2015). Modeling geomagnetic cutoffs for space weather applications. *Journal of Geophysical Research: Space Physics*, 120, 5694–5702. <https://doi.org/10.1002/2014JA020899>
- Kress, B. T., Hudson, M. K., & Slocum, P. L. (2005). Impulsive solar energetic ion trapping in the magnetosphere during geomagnetic storms. *Geophysical Research Letters*, 32, L06108. <https://doi.org/10.1029/2005GL022373>
- Kress, B., Mertens, C., & Wiltberger, M. (2010). Solar energetic particle cutoff variations during the 29–31 October 2003 geomagnetic storm. *Space Weather*, 8, S05001. <https://doi.org/10.1029/2009SW000488>
- Kress, B., Rodriguez, J., Mazur, J., & Engel, M. (2013). Modeling solar proton access to geostationary spacecraft with geomagnetic cutoffs. *Advances in Space Research*, 52(11), 1939–1948. <https://doi.org/https://doi.org/10.1016/j.asr.2013.08.019>
- Leske, R., Mewaldt, R., Stone, E., & Rosengvinge, T. (2001). Observations of geomagnetic cutoff variations during solar energetic particle events and implications for the radiation environment at the space station. *Journal of Geophysical Research*, 106(A12), 30,011–30,022. <https://doi.org/10.1029/2000JA000212>
- Li, X., Baker, D. N., Kanekal, S. G., Looper, M., & Temerin, M. (2001). Long term measurements of radiation belts by SAMPEX and their variations. *Geophysical Research Letters*, 28(20), 3827–3830. <https://doi.org/10.1029/2001GL013586>
- Lorentzen, K. R., Mazur, J. E., Looper, M. D., Fennell, J. F., & Blake, J. B. (2002). Multisatellite observations of MeV ion injections during storms. *Journal of Geophysical Research*, 107(A9), SMP 7–1–SMP 7–11. <https://doi.org/10.1029/2001JA000276>
- Luhmann, J. G., Mays, M. L., Li, Y., Lee, C. O., Bain, H., Odstrcil, D., et al. (2018). Shock connectivity and the late cycle 24 solar energetic particle events in July and September 2017. *Space Weather*, 16, 557–568. <https://doi.org/10.1029/2018SW001860>
- Mazur, J., Friesen, L., Lin, A., Mabry, D., Katz, N., Dotan, Y., et al. (2013). The Relativistic Proton Spectrometer (RPS) for the Radiation Belt Storm Probes Mission. *Space Science Reviews*, 179(1), 221–261. <https://doi.org/10.1007/s11214-012-9926-9>
- Miyoshi, Y., Morioka, A., Misawa, H., Obara, T., Nagai, T., & Kasahara, Y. (2001). Rebuilding process of the outer radiation belt during the 3 November 1993 magnetic storm: NOAA and Exos-D observations. *Journal of Geophysical Research*, 108(A1), SMP 3–1–SMP 3–15. <https://doi.org/10.1029/2001JA007542>
- O'Brien, T. P., Mazur, J. E., & Looper, M. D. (2018). Solar energetic proton access to the magnetosphere during the 10–14 September 2017 particle event. *Space Weather*, 16, 2022–2037. <https://doi.org/10.1029/2018SW001960>
- Ogliore, R. C., Mewaldt, R. A., Leske, R. A., Stone, E. C., & von Rosengvinge, T. T. (2001). A direct measurement of the geomagnetic cutoff for cosmic rays at space station latitudes. In *Proceedings of the 27th International Cosmic Ray Conference*, 10, Hamburg, Germany, pp. 4112.
- Qin, M., Zhang, X., Ni, B., Song, H., Zou, H., & Sun, Y. (2014). Solar cycle variations of trapped proton flux in the inner radiation belt. *Journal of Geophysical Research: Space Physics*, 119, 9658–9669. <https://doi.org/10.1002/2014JA020300>
- Rodriguez, J. V., Onsager, T. G., & Mazur, J. E. (2010). The east-west effect in solar proton flux measurements in geostationary orbit: A new GOES capability. *Geophysical Research Letters*, 37, L07109. <https://doi.org/10.1029/2010GL042531>
- Selesnick, R. (2014). Optimal performance of charged particle telescopes in space. *Nuclear Instruments and Methods in Physics Research Section A: Accelerators, Spectrometers, Detectors and Associated Equipment*, 761, 34–38. <https://doi.org/https://doi.org/10.1016/j.nima.2014.05.109>
- Selesnick, R. S., Baker, D. N., Jaynes, A. N., Li, X., Kanekal, S. G., Hudson, M. K., & Kress, B. T. (2014). Observations of the inner radiation belt: CRAND and trapped solar protons. *Journal of Geophysical Research: Space Physics*, 119, 6541–6552. <https://doi.org/10.1002/2014JA020188>
- Selesnick, R. S., Baker, D. N., Jaynes, A. N., Li, X., Kanekal, S. G., Hudson, M. K., & Kress, B. T. (2016). Inward diffusion and loss of radiation belt protons. *Journal of Geophysical Research: Space Physics*, 121, 1969–1978. <https://doi.org/10.1002/2015JA022154>
- Selesnick, R., Baker, D., & Kanekal, S. (2017). Proton straggling in thick silicon detectors. *Nuclear Instruments and Methods in Physics Research Section B: Beam Interactions with Materials and Atoms*, 394, 145–152. <https://doi.org/https://doi.org/10.1016/j.nimb.2017.01.028>
- Selesnick, R. S., Baker, D. N., Kanekal, S. G., Hoxie, V. C., & Li, X. (2018). Modeling the proton radiation belt with Van Allen probes relativistic electron-proton telescope data. *Journal of Geophysical Research: Space Physics*, 123, 685–697. <https://doi.org/10.1002/2017JA024661>
- Selesnick, R., Hudson, M., & Kress, B. (2010). Injection and loss of inner radiation belt protons during solar proton events and magnetic storms. *Journal of Geophysical Research*, 115, A08211. <https://doi.org/10.1029/2010JA015247>
- Selesnick, R. S., Looper, M. D., & Mewaldt, R. A. (2007). A theoretical model of the inner proton radiation belt. *Space Weather*, 5, S04003. <https://doi.org/10.1029/2006SW000275>
- Shen, X.-C., Hudson, M. K., Jaynes, A. N., Shi, Q., Tian, A., Claudepierre, S. G., et al. (2017). Statistical study of the storm time radiation belt evolution during Van Allen probes era: CME- versus CIR-driven storms. *Journal of Geophysical Research: Space Physics*, 122, 8327–8339. <https://doi.org/10.1002/2017JA024100>
- Spence, H. E., Reeves, G. D., Baker, D. N., Blake, J. B., Bolton, M., Bourdarie, S., et al. (2013). Science goals and overview of the radiation belt storm probes (RBSP) energetic particle, composition, and thermal plasma (ECT) Suite on NASA's Van Allen Probes Mission. *Space Science Reviews*, 179(1), 311–336. <https://doi.org/10.1007/s11214-013-0007-5>
- Störmer, C. (1955). *The polar aurora*. Oxford: Clarendon Press.
- Tsyganenko, N., & Sitnov, M. (2005). Modeling the dynamics of the inner magnetosphere during strong geomagnetic storms. *Journal of Geophysical Research*, 110, A03208. <https://doi.org/10.1029/2004JA010798>
- Zou, H., Zong, Q. G., Parks, G. K., Pu, Z. Y., Chen, H. F., & Xie, L. (2011). Response of high-energy protons of the inner radiation belt to large magnetic storms. *Journal of Geophysical Research*, 116, A10229. <https://doi.org/10.1029/2011JA016733>